ChemComm

Accepted Manuscript

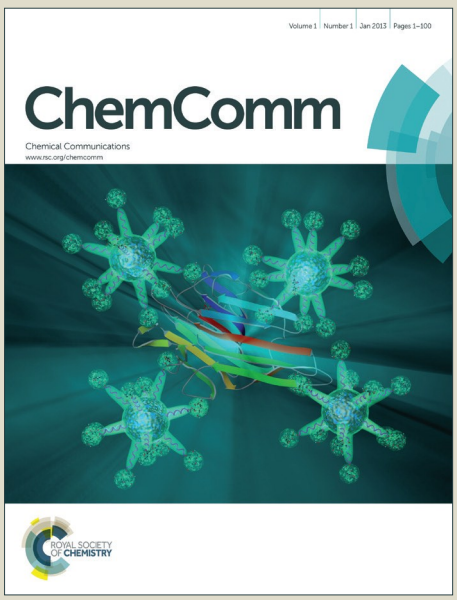

This is an *Accepted Manuscript*, which has been through the Royal Society of Chemistry peer review process and has been accepted for publication.

Accepted Manuscripts are published online shortly after acceptance, before technical editing, formatting and proof reading. Using this free service, authors can make their results available to the community, in citable form, before we publish the edited article. We will replace this *Accepted Manuscript* with the edited and formatted *Advance Article* as soon as it is available.

You can find more information about *Accepted Manuscripts* in the Information for Authors.

Please note that technical editing may introduce minor changes to the text and/or graphics, which may alter content. The journal's standard Terms & Conditions and the Ethical guidelines still apply. In no event shall the Royal Society of Chemistry be held responsible for any errors or omissions in this *Accepted Manuscript* or any consequences arising from the use of any information it contains.

ROYAL SOCIETY OF CHEMISTRY

www.rsc.org/chemcomm

Please do not adjust margins

ChemCommun

COMMUNICATION

Hydrophilic non-precious metal nitrogen-doped carbon electrocatalysts for enhanced efficiency in oxygen reduction reaction

Received 00th January 20xx,

Accepted 00th January 20xx

DOI: 10.1039/x0xx00000x

www.rsc.org/

Guang-Ping Hao,[a] Nastaran Ranjbar Sahraie,[b] QiangZhang,[c] Simon Krause,[a] Martin Oschatz,[a] Alicja Bachmatiuk,[d,e] Peter Strasser*[b] and Stefan Kaskel*[a,f]

Exploring the role of surface hydrophilicity of non-precious metal N-doped carbon electrocatalysts on electrocatalysis is challenging. Herein we discover an ultra-hydrophilic non-precious carbon electrocatalyst, showing enhanced catalysis efficiency on both gravimetric and surface area basis for oxygen reduction reaction due to a high dispersion of active centres.

The oxygen reduction reaction (ORR) is a fundamental electrochemical reaction for fuel cells and metal-air batteries. ORR research has long been focused on the development and understanding of new non-precious nitrogen-doped carbon catalysts that result in significant cost reduction by platinum metal substitution. To catalyze broader commercialization of such devices and technologies, efficient and affordable non-precious electrocatalysts will ultimately be required. One of the most prominent examples is pyrolyzed solid materials consisting of non-precious metal/nitrogen/carbon (M/N/C-) composites,[1] or metal-free, heteroatom-doped nanocarbons.[2] The nature of the active sites in term of the modulation of electron donating/withdrawing of carbon basal plane by incorporated heteroatoms of the M/N/C electrocatalysts has been under intensive investigations and become more and more clear.[3] However, a detailed understanding of the effect of surface hydrophilicity and wettability on the dispersion of metal-related active sites as well as their effects on catalysis efficiency of the M/N/C materials has remained elusive.

On the one hand, a hydrophilic pore surface benefits a facile loading and a high dispersion of active metal-related species, because a hydrophilic affinity can be created between hydrophilic pore walls and precursors, and further inhibits precursor random migration and agglomeration.[4] On the other hand, a hydrophilic pore surface may also influence the transport of hydrated O_2 to the electrochemically active centres under hydrated conditions, finally affecting the activity.[5] To our knowledge, such effects stemmed from surface hydrophilicity have been rarely investigated to date.

Taking these into consideration, in this contribution, we surface engineered a number of different carbon-based materials with surface characteristics ranging from an ultra-hydrophilic carbon network to an ultra-hydrophobic carbon black. We observe that hydrophilicity, quantified by water adsorption isotherms at 298 K, is correlated with much enhanced ORR catalysis efficiency.

Firstly, a group of ultra-hydrophilic electrocatalysts (Fe/N_1/3.2, Fe/Cu/N_1.3/1/8, and Cu/N_1/4, according to the nominal atomic ratio of Fe/N, Fe/Cu/N and Cu/N in the synthesis, Fig. 1a-c) were fabricated by a facile and scalable impregnation and subsequent pyrolysis and leaching method (Experimental section, ESI†) based on an unprecedented, hydrophilic carbon network (DUT-110, DUT = Dresden University of Technology, derived from a functional complex[6]. The highly hydrophilic surface property of DUT-110 was confirmed by the sharp uptake in water vapor adsorption isotherm from very beginning, showing a record value until P/P_0<0.3 (Fig. S1a, ESI†).[7] The narrow and rich micropores were proven by its type I isotherm and pore size distribution based on N_2 physisorption data (Fig. S1b, ESI†) as well as high

[a] Department of Inorganic Chemistry, TechnischeUniversität Dresden, Bergstraße 66, 01069 Dresden, Germany.
E-mail: Stefan.Kaskel@chemie.tu-dresden.de
[b] The Electrochemical Energy, Catalysis, and Materials Science Laboratory, Department of Chemistry, Chemical Engineering Division, Technical University Berlin, Straße des 17. Juni 124, 10623 Berlin, Germany.
E-mail: pstrasser@tu-berlin.de
[c] Beijing Key Laboratory of Green Chemical Reaction Engineering and Technology, Department of Chemical Engineering, Tsinghua University, Beijing 100084, P. R. China.
[d] IFW Dresden, Institute of Complex Materials, P. O. Box 270116, D-01171, Dresden, Germany.
[e] Center of Polymer and Carbon Materials, Polish Academy of Sciences, M. Curie-Sklodowskiej 34, Zabrze 41-819, Poland.
[f] Fraunhofer Institute for Material and Beam Technology, Winterbergstraße 28, 01277, Dresden, Germany.
† Electronic Supplementary Information (ESI) available. See
DOI: 10.1039/x0xx00000x

ChemComm Accepted Manuscript

Please do not adjust margins

resolution TEM images (Fig. S1c, ESI†); while the STEM mapping and XPS spectrum revealed the highly heteroatom-doped feature, with a surface composition of C, N, and O with the atomic content of 74.7, 14.3, and 10.33%, respectively (Fig. S1d, e, ESI†). In parallel, the hydrophobic non-precious electrocatalysts were prepared under the same principle through modification of N-containing polymers (polyaniline, PANI or N-containing ionic liquid, N, N-ethyl-methyl-imidazolium-dicyanamide) and $FeCl_3$, but based on highly hydrophobic carbon black (Ketjen EC 600J). To note, the pyrolysis and leaching treatment as well as the following performance evaluation were kept identical with that of the hydrophilic groups.

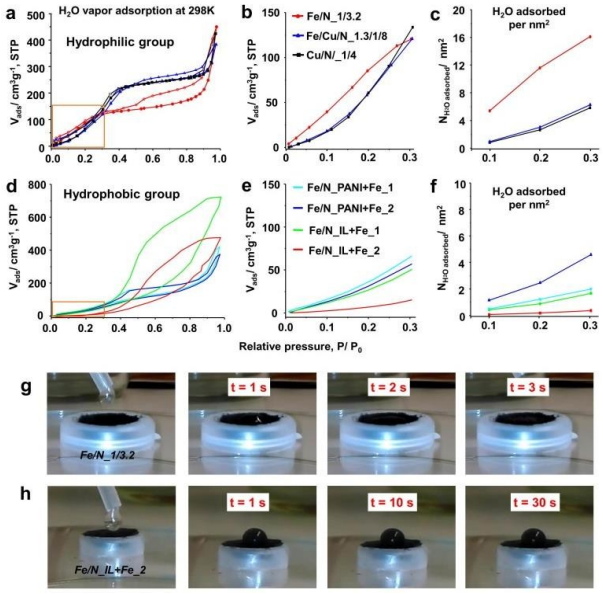

Fig. 1 H_2O vapor adsorption isotherm at different relative pressure range at 298 K of hydrophilic groups (a-c) and hydrophobic groups (d-f), (g, h) Comparison of dynamic water contact angle changes of typical samples of the two group.

Surprisingly, the final hydrophilic electrocatalysts, Fe/N_1/3.2, Fe/Cu/N_1.3/1/8, and Cu/N_1/4, maintained largely the high surface hydrophilicity. They all exhibit relatively high hydrophilic properties, with the water uptake of 120.4, 120.5, and 133.6 cm^3g^{-1} (equivalent to 5.37, 5.38, and 5.96 $mmolg^{-1}$) at P/P_0=0.3 for Fe/N_1/3.2, Fe/Cu/N_1.3/1/8, and Cu/N_1/4, respectively (Fig. 1a). The water adsorption behavior in the range of $0<P/P_0<0.3$ is mainly determined by surface hydrophilicity,[7] thus we further compared the water sorption uptake in this pressure range (Fig. 1b). All the hydrophilic samples, i.e., Fe/N_1/3.2, Fe/Cu/N_1.3/1/8, and Cu/N_1/4, exhibits a higher water adsorption uptake, even though their less developed porosity and low surface area (200-574 m^2g^{-1}, Fig. S2, ESI†) compared to hydrophobic materials (340-1079 m^2g^{-1}, Table S1, ESI†). After normalizing to specific surface area (Fig. 1c), the hydrophilicity order is Fe/N_1/3.2 > Fe/Cu/N_1.3/1/8 > Cu/N_1/4. For instance, the water adsorption uptake is calculated to be 16.2 H_2O molecules/nm^2, 6.7 H_2O molecules/nm^2 and 6.2 H_2O molecules/nm^2 at P/P_0=0.3 for Fe/N_1/3.2, Fe/Cu/N_1.3/1/8, and Cu/N_1/4, respectively. However, the water adsorption isotherm of hydrophobic electrocatalysts display much lower water adsorption uptakes, indicating a much lower surface hydrophilicity (Fig. 1d-f). To illustrate the difference in hydrophilicity vividly, the water contact angle was recorded dynamically after water droplets contacted the carbon pellet and compared (herein we show the sample of Fe/N_1/3.2 and Fe/N_IL+Fe_2 as Fig. 1g, h). For the hydrophilic Fe/N_1/3.2, the water droplet can be adsorbed in 3 s with a final contact angle of *ca*. 0; while sample of Fe/N_IL+Fe_2 was not wetted until 30 s, again confirming the distinct surface hydrophilicity. Morphologically, the hydrophilic electrocatalysts all exhibit a highly interconnected network structure (Fig. S3, ESI†), but much denser structure comparing with their host carbon networks DUT-110 (Fig. S1d, ESI†). This is due to the shrinkage of carbon skeletons during high temperature pyrolysis.

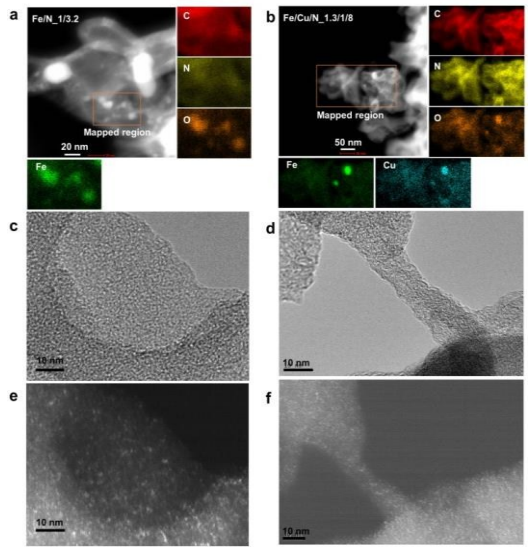

Fig. 2 STEM maps of Fe/N_1/3.2 (a) and Fe/Cu/N_1.3/1/8 (b), TEM image and the corresponding dark-field TEM image of Fe/N_1/3.2 (c, e) and Fe/Cu/N_1.3/1/8 (d, f).

Based on the unique hydrophilicity and narrow micropores, a high dispersion of metal-related nanoparticles was expected for hydrophilic electrocatalysts. Thus, the elemental distribution was analysed by STEM images and elemental maps as well as dark-field TEM images (Fig. 2). For Fe/N_1/3.2 (Fig. 2a), large and bright particles can be observed, while for Fe/Cu/N_1.3/1/8, only very few isolated particles can be detected (Fig. 2b). This observation is consistent with the TEM images (Fig. S4, ESI†). Importantly, except some large particles, the distribution of small metal species is very homogeneous, indicating highly dispersed nanoclusters or even mononuclear metal species embedded in the carbon matrix. The dark-field TEM images (Fig. 2e, f), corresponding to their relevant TEM images (Fig. 2c, d) again confirmed a high and uniform distribution of metal-related nanoclusters over the whole framework. The metal content determined by ICP technique is 3.8 wt% Fe for Fe/N_1/3.2 and 1.22 wt% Fe for

ChemComm Accepted Manuscript

This journal is © The Royal Society of Chemistry 20xx
Please do not adjust margins

Please do not adjust margins

Fe/N_1/3.2. To note, these metal nanoclusters should be tightly embedded in the carbon matrix, since all these electrocatalysts have been extensively leached in 2.0 M H_2SO_4 at 110 ^oC for 24 h before harvest for characterisation and application. Furthermore, the hybrid structure composed of graphitic domains and amorphous carbons was revealed by Raman spectra (Fig. S5, fitting details in Table S2, ESI†) with the I_D/I_G ratio of 1.55, 1.82 and 2.11 for Fe/N_1/3.2, Fe/Cu/N_1.3/1/8 and Cu/N_1/4, respectively, confirming observation by TEM images (Fig. S4, ESI†).

For non-metal elements such as C, O, and N, a homogeneous dispersion was also observed by elemental maps (Fig. 2a,b), indicating a uniform doped structure. Interestingly, comparing the Fe or Cu maps with O maps, a strong relevance is found between metal and O, particularly for large particles, indicating their oxide phase in nature. This observation is further confirmed by their XPS analysis (Fig. S6, ESI†). Furthermore, Table S1 (ESI†) also listed other structural parameters such as specific surface area analyzed by N_2 adsorption, surface non-metal compositions determined by XPS and metal species detected by ICP for all the hydrophilic and hydrophobic catalysts groups in order to get a reliable correlation between structural parameters and the following catalysis performance.

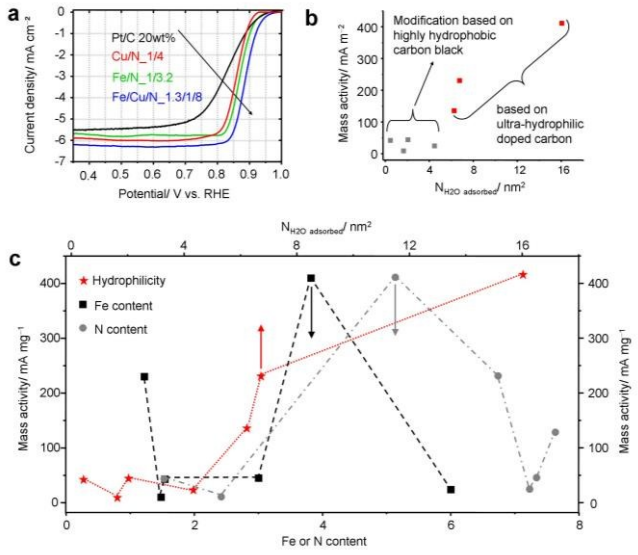

Fig. 3 ORR catalysis evaluation in O_2-saturated 0.10 M KOH. (a) Linear sweep voltammetry (LSV) ORR plots under conditions of room temperature, rotating speed of 1500 rpm, scan rate of 10 mV s^{-1}, the non-precious catalysts loading of 0.80 mg cm^{-2}, and the benchmark Pt loading of 10 μg cm^{-2}. (b) The relationship between hydrophilicity in term of water molecules adsorbed per nm^2 based on water adsorption data at P/P_0=0.3 and mass activity. (c) structure-performance comparison including surface hydrophilicity, nitrogen content (atomic%, by XPS) and Fe content (wt.%, by ICP) with mass activity in ORR electrocatalysis under identical conditions.

We first evaluated the ORR activity of the hydrophilic group, *i.e.*, Fe/N_1/3.2, Fe/Cu/N_1.3/1/8, and Cu/N_1/4. Linear sweep voltammetry (LSV, Fig. 3a) in 0.10 M KOH was employed to investigate the catalytic activity of the catalysts compared to Pt/C benchmark catalysts. The onset potential (E_{onset}, noteworthy onset potential is defined as the potential at which the current density reaches 1.0 $mAcm^{-2}$) are 0.90, 0.92, and 0.89 V for Fe/N_1/3.2, Fe/Cu/N_1.3/1/8, and Cu/N_1/4, respectively (Fig. 3a, Table S1, ESI†). The E_{onset} of Fe/Cu/N_1.3/1/8 is positive and comparable with the reported state-of-the-art non-precious catalysts such as Fe/N-doped nanocarbons (*e.g.* N-CNT/Fe_3C, N-doped carbon nanoplate/Fe_3C, Fe@Fe_3C/N-doped carbon),[8] Fe and/or N-doped porous carbons with higher surface area or larger pores such as mesopores [9] or hierarchical pores,[10] and the hybrid N-Fe-CNT/carbon nanoparticle with higher Fe content.[11] The half-wave potential ($E_{1/2}$) shows similar trend that is also comparable with the state-of-the-art non-precious electrocatalysts (Table S3, ESI†).[9-12] Particularly, the high activity reflected by the positive E_{onset} and $E_{1/2}$ of Fe/Cu/N_1.3/1/8 originates from the highly dispersed active sites and highly accessible porosity.

The mass activity indicates the utilization efficiency of catalysts on gravimetric basis. For the hydrophilic series relatively higher mass activities up to 413.3, 232.5, and 137.7 $mAmg^{-1}$ were calculated for Fe/N_1/3.2, Fe/Cu/N_1.3/1/8, and Cu/N_1/4, respectively (Fig. 3b). For the hydrophobic samples, the mass activity is one order of magnitude lower (Fig. 3b). The much higher mass activity for hydrophilic samples originated from the positively shifted onset and half-wave potential, indicating the large density of accessible active sites due to the high dispersion of electrochemically active sites benefited from the high hydrophilic carbon surface. In order to understand quantitatively, we further normalized the mass activity by their surface area. The obtained specific activities are 2067, 482.4, and 239.9 mAm^{-2} for Fe/N_1/3.2, Fe/Cu/N_1.3/1/8, and Cu/N_1/4, respectively. This trend is also consistent with that of mass activity, reflecting the remarkable high surface efficiency (Fig. S7, Table S1, ESI†).

Moreover, we correlated the Fe and N content, the surface area as well as surface hydrophilicity with mass activity. However, it is difficult to find a clear trend between either mass or specific activity with doping properties (Fig. 3c, black and grey line, Fig. S8 ESI†) or specific surface area (Table S1, Fig. S9 ESI†). In contrast, a clear correlation between mass activity and surface hydrophilicity was observed. This probably because 1) the higher surface hydrophilicity induces higher dispersion of active sites, 2) hydrophilic pores benefit an easy accessibility to the active sites of reactants (such as hydrated O_2 as ORR proceeds). Besides the comparison between specific samples, the comparison between hydrophobic group and ultra-hydrophilic group confirmed the same rule (Fig. 3c, red trend line).

The high dispersion of active sites benefiting from surface hydrophilicity has been proven above by STEM mapping and dark field TEM images. However, to observe the effect of hydrophilicity on the diffusion of hydrated O_2 and resultant H_2O is challenging. For the diffusion of hydrated O_2 near reaction interfaces, a high surface hydrophilicity may be

ChemComm Accepted Manuscript

Please do not adjust margins

beneficial.[5b-d] In order to explain this point, we hypothesized a "physical structure" (Fig. S10, ESI†), where water molecules around hydrated O_2 molecules can be readily stripped by the hydrophilic micropore walls when approaching the carbon slit pores, then the liberated O_2 molecules can freely diffuse to the active sites and thus accelerate the reaction. The O_2 adsorption was investigated for the active hydrophilic group, which can give the first clue that a high surface hydrophilicity enhanced the O_2 adsorption (Fig. S11, ESI†). All hydrophilic samples exhibit a combined type I isotherm (Fig. S9a,b ESI†), indicating a strong interaction between O_2 molecules and doped carbon pore walls. After normalized by the specific surface area, the samples showed a higher areal uptake, indicating the preferential O_2 adsorption and high surface utilization efficiency for trapping O_2 molecules (Fig. S11c, ESI†). Interestingly, the O_2 capture behaviour is consistent to that of water sorption in the same pressure range.

In addition, one would realize that the high surface hydrophilicity of the catalysts may also cause the delay of water desorption when used for applications that generate water such as alkaline fuel cells (AFC). In this case, further H_2 reduction can be applied to effectively reduce surface hydrophilicity (Fig. S12, ESI†). Through this way, the possible flooding issues can be avoided in potential applications such as AFC.

In summary, exemplified using the non-precious carbon based ORR electrocatalyst concept, we surface engineered a number of different carbon based materials with surface characteristics ranging from an ultra-hydrophilic carbon network to an ultra-hydrophobic carbon black. A high surface hydrophilicity has been found to form an easily wetted surface which first ensures a high dispersion of metal-related active sites and may also increase the accessibility of reactants to active centres, and thus increase surface and mass utilization efficiency of catalysts. This work provides fresh insight in the controlling materials parameters of non-precious ORR catalysts, and as such offers new clues and strategies on how to increase the ORR catalysis efficiency by tuning surface chemistry of non-precious electrocatalysis. The insight on hydrophilicity may also be important to other heterogeneous catalytic reactions such as CO_2 electro-reduction, glucose oxidation, metal-air batteries etc catalyzed on hydrated carbon surfaces.

We thank Prof. A. Eychmüller and S. Klosz for Raman spectra measurement, Dr. I. Senkovska for help in the O_2 adsorption measurement. G.-P. H. acknowledges the financial support from Alexander von Humboldt Foundation.

Notes and references

1 (a) M. Lefèvre, E. Proietti, F. Jaouen and J-P. Dodelet, *Science,* 2009, **324**, 71; (b) F. Jaouen, E. Proietti, M. Lefèvre, R. Chenitz, J.-P. Dodelet, G. Wu, H. T. Chung, C. M. Johnston and P. Zelenay, *Energy Environ. Sci.,* 2011, **4**, 114; (c) G. Wu, K. L. More, C. M. Johnston and P. Zelenay, *Science,* 2011, **332**, 443; (d) M. K. Debe, *Nature,* 2012, **486**, 43; (e) K. Wood, R. O'Hayre and S. Pylypenko, *Energy Environ. Sci.,* 2014, **7**, 1212; (f) D.-W. Wang and D. Su, *Energy Environ. Sci.,* 2014, **7**, 576; (g) G. Wu and P. Zelenay, *Acc. Chem. Res.,* 2013, [illegible], 1878.

2 (a) K. Gong, F. Du, Z. Xia, M. Durstock and L. Dai, *Science,* 2009, **323**, 760; (b) L. Qu, Y. Liu, J.-B. Baek and L. Dai, *ACS Nano,* 2010, **4**, 1321; (c) W. Wei, H. Liang, K. Parvez, X. Zhuang and X. Feng, K. Müllen, *Angew. Chem. Int. Ed.,* 2014, **53**, 1570; (d) Y. Jiao, Y. Zheng, M. Jaroniec and S. Z. Qiao, *J. Am. Chem. Soc.,* 2014, **136**, 4394; (e) J. Liang, Y. Jiao, M. Jaroniec and S. Z. Qiao, *Angew. Chem. Int. Ed.,* 2012, **51**, 11496. (f) D. Yu, Q. Zhang and L. Dai, *J. Am. Chem. Soc.,* 2010, **132**, 15127.

3 (a) J-L. Shui, N. K. Karan, M. Balasubramanian, S-Y. Li, and D-J. Liu, *J. Am. Chem. Soc.,* 2012, **134**, 16654. (b) N. Ramaswamy, U. Tylus, Q. Jia and S. Mukerjee, *J. Am. Chem. Soc.,* 2013, **135**, 15443; (c) Y. Zhu, B. Zhang, X. Liu, D.-W. Wang And D. Su. *Angew. Chem. Int. Ed.,* 2014, **53**, 10673; (d) U. I. Kramm, M. Lefèvre, N. Larouche, D. Schmeisser and J.-P. Dodelet, *J. Am. Chem. Soc.,* 2014, **136**, 978; (e) C. H. Choi, H. K. Lim, M. W. Chung, J. C. Park, H. Shin, H. Kim and S. I. Woo, *J. Am. Chem. Soc.,* 2014, **136**, 9070.

4 (a) A.-H. Lu and F. Schüth, *Adv. Mater.,* 2006, **18**, 1793; (b) Y. Yang and D. Zhao, *J. Mater. Chem.*, 2005, **15**, 1217; (c) Q. Wang, Z.-Y. Zhou, Y.-J. Lai, Y. You, J-G. Liu, X.-L. Wu, E. Terefe, C. Chen, L. Song, M. Rauf, N. Tian, S.-G. Sun, *J. Am. Chem. Soc.,* 2014, **136**, 10882.

5 (a) S. Holdcroft, *Chem. Mater.,* 2014, **26**, 381; (b) D. Yu, E. Nagelli, F. Du and L. Dai, *J. Phys. Chem. Lett. ,* 2010, **1**, 2165; (c) G. J. Sohn, H. J. Choi, I. Y. Jeon, D. W. Chang, L. Dai and J. B. Baek, *ACS Nano,* 2012, **6**, 6345; (d) I. Y. Jeon, H. J. Choi, S. M. Jung, J. M. Seo, M. J. Kim, L. Dai and J. B. Baek, *J. Am. Chem. Soc.,* 2013, **135**, 1386.

6 (a) G.-P. Hao, G. Mondin, Z. Zheng, T. Biemelt, S. Klosz, F. Schubel, A. Eychmüller and S. Kaskel, *Angew. Chem. Int. Ed.,* 2015, **54**, 1941; (b) K. Kaneko, *Nature Chem.*, 2015, **7**, 194.

7 (a) D. D. Do, S. Junpirom, H. D. Do, *Carbon,* 2009, **47**, 1466; (b) T. Matsuoka, H. Hatori, M. Kodama and J. Yamashita, N. Miyajima, *Carbon*, 2004, **42**, 2329; (c) J. K. Brennan, K. T. Thomson and K. E. Gubbins, *Langmuir*, 2002, **18**, 5438; (d) H.-J. Wang, A. Kleinhammes, T. P. McNicholas, J. Liu and Y. J. Wu, *J Phys. Chem. C,* 2014, **118**, 8474; (e) Y. Tao, M. Endo and K. Kaneko, *J. Am. Chem. Soc.*, 2009, **131**, 904; (f) T. Ohba and K. Kaneko, *J. Phys. Conf. Ser.*, 2009, **177**, 012001.

8 (a) W. Yang, X. Liu, X. Yue, J. Jia and S. Guo, *J. Am. Chem. Soc.,* 2015, **137**, 1436; (b) S. Zhao, H. Yin, L. Du, L. He, K. Zhao, L. Chang, G. Yin, H. Zhao, S. Liu and Z. Tang, *ACS Nano,* 2014, **8**, 12660; (c) K. Ai, Y. Liu, C. Ruan, H. Lu and G. Lu, (Max), *Adv. Mater.,* 2013, **25**, 998.

9 (a) Z. Li, G. Li, L. Jiang, J. Li, G. Sun, C. Xia and F. Li, *Angew. Chem. Int. Ed.,* 2015, **54**, 1494; (b) R. Liu, D. Wu, X. Feng and K. Müllen, *Angew. Chem. Int. Ed.,* 2010, **49**, 2565.

10 (a) H.-W. Liang, X. Zhuang, S. Brüller, X. Feng and K. Müllen, *Nat. Commun.*, 2014, **5**, 4973; (b) G-L. Tian, M-Q. Zhao, D. Yu, X-Y. Kong, J-Q. Huang, Q. Zhang and F. Wei, *Small,* 2014, **10**, 2251.

11 H. T. Chung, J. H. Won and P. Zelenay, *Nat. Commun.*, 2013, **4**, 1922.

12 (a) S. Zhao, H. Yin, L. Du, L. He, K. Zhao, L. Chang, G. Yin, H. Zhao, S. Liu and Z. Tang, *ACS Nano,* 2014, **8**, 12660; (b) W. Yang, X. Liu, X. Yu and J. Jia, S. Guo, *J. Am. Chem. Soc.* 2015, **137**, 1436; (c) N. R. Sahraie, J. P. Paraknowitsch, C. Göbel and A. Thomas, P. Strasser, *J. Am. Chem. Soc.* 2014, **136**, 14486.

ChemComm Accepted Manuscript

This journal is © The Royal Society of Chemistry 20xx